Experimental comparison of HFO-1234ze(E) and R-515B to replace HFC-134a in heat pump water heaters and moderately high temperature heat pumps

Adrián Mota-Babiloni [*], Carlos Mateu-Royo, Joaquín Navarro-Esbrí, Ángel Barragán-Cervera

ISTENER Research Group, Department of Mechanical Engineering and Construction, Universitat Jaume I (UJI), Castelló de la Plana, E-12071, Spain

ARTICLE INFO

ABSTRACT

Heat pumps are gaining interest to replace fossil fuel burners with the increase of the share of renewable sources in the electricity generation mix. Moreover, low global warming potential (GWP) alternatives offer a more environmentally friendly option as refrigerants. HFO-1234ze(E) and its non-flammable mixture R-515B are experimentally investigated for the first time to replace HFC-134a in heat pump water heaters (HPWH) and moderately high temperature heat pumps (MHTHP). Tests are performed in a test rig equipped with a variable frequency compressor at evaporating temperatures of 7.5, 15 and 22.5 °C and condensing temperatures from 55 to 85 °C (65 experimental tests). HFC-134a outperforms both alternatives in heating capacity (approx. 26% higher) due to the higher mass flow rate and heating effect. However, this effect is compensated by, on average, 25% lower compressor power consumption. Therefore, the coefficient of performance (COP) is comparable or slightly higher (up to 5%) for HFO-1234ze(E) and R-515B. Considering the positive results in COP and the reduced GWP, both options decrease HFC-134a MHTHP equivalent carbon emissions down to 28%. Besides, given the 20 K lower discharge temperature reached by the alternatives, the compressor operating map can be significantly extended. Finally, it is demonstrated that R-515B is a suitable non-flammable alternative to HFO-1234ze(E) that keep energetic and environmental benefits while offers a safer system operation.

1. Introduction

As renewable energies increase their energy mix presence, heat pumps appear as an environmentally friendly replacement for fossil fuels in several applications. The interest in this technology is increasing [1]. However, alternative refrigerants for heat pump water heater (HPWH) and moderately high temperature heat pumps (MHTHP) have not been studied yet in deep, contrary to other applications such as commercial refrigeration [2,3], domestic refrigeration [4], domestic air conditioners heat pumps [5], or even very high temperature heat pumps [6,7]. HPWH and MHTHP can be used in several applications, including domestic, commercial or industrial sectors [8].

During the past years, research has been focused on the use of CO_2 (R-744) in optimised heat pumps [9]. Besides, environmentally friendly hydrocarbon refrigerants are classified as highly toxic fluids by the ASHRAE. Then, hydrofluorocarbons (HFC), typically used in other applications, could be an alternative. Still, their phase-out and phase-down have been defined by the Kigali Amendment [10].

HPWH and MHTHP can have various suitable working fluids, depending on the temperature level. For instance, synthetic mixtures have been proposed to replace R410A water-to-water heat pumps [11,12]. Besides, for HFC-134a operating levels, other replacements could be considered to design an energy-efficient system with higher safety and reliability [13]. In this way, two solutions are proposed, pure and mixed HFOs.

The main characteristics of HFO-1234ze(E) for HFC-134a replacement were exposed by Mota-Babiloni et al. [14]. On the one hand, HFO-1234ze(E) requires larger compressor displacement for a match in cooling/heating capacity, and flammability could represent a problem in specific applications. On the other hand, HFO-1234ze(E) energetic performance is comparable or even higher than HFC-134a, and its heat transfer performance is appealing. Another interesting feature of the alternative refrigerant HFO-1234ze(E) is the higher critical temperature than HFC-134a and other alternative HFCs and HFOs (such as HFO-1234yf). For example, He et al. [15] included HFO-1234ze(E) in the list of candidates for the vapour compression subsystem of a two-stage absorption-compression cascade refrigeration system. Compared to

---

Nomenclature

COP	coefficient of performance
c_p	specific heat capacity (kJ kg^{-1} K^{-1})
E_a	annual electric energy consumption (kWh year^{-1})
h	enthalpy (kJ kg^{-1})
L	leakage ratio (%)
$\dot{m}$	mass flow rate (kg s^{-1})
m	mass of refrigerant (kg)
n	lifetime of the heat pump system (years)
N	rotational speed (rpm)
$\dot{Q}_k$	heating capacity (kW)
T	temperature (°C)
V	volume (m^3)
$\dot{W}$	compressor power consumption (kW)

Greek

α	Refrigerant recovered (%)
β	Carbon emission factor (gCO$_2$e kWh^{-1})
ε	thermal effectiveness
ρ	density (kg m^{-3})
η	efficiency

Subscripts

c	compressor

ev	evaporator
in	inlet
is	isentropic
k	condenser
out	outlet
ref	refrigerant
suc	suction
vol	volumetric

Abbreviatures

ASHRAE	American Society of Heating, Refrigerating and Air-Conditioning Engineers
GWP	global warming potential (100 years)
HFC	hydrofluorocarbon
HFO	hydrofluoroolefin
HPWH	heat pump water heater
HTHP	heat temperature heat pump
MHTHP	moderately high temperature heat pump
IHX	internal heat exchanger
NBP	normal boiling point
PID	proportional-integrative-derivative
POE	polyolester oil
ODP	ozone depletion potential
TEWI	total equivalent warming impact

HFC-134a (and other HFCs and HFO-1234yf), HFO-1234ze(E) COP highlighted at increasing operating temperatures. HFO-1234ze(E) outperforms HFO-1234yf and HFC-134a at high vapour qualities (if the heat flux is sufficiently low or the mass velocity is adequately high), while its performance is the lowest at low vapour qualities [16].

Nawaz et al. [17] recommended using HFO-1234yf and HFO-1234ze(E) as alternatives to HFC-134a in HPWH (average production temperature 52 °C). They combined different condenser wrap patterns, condenser tube sizes, tank insulation effectiveness, and evaporator sizes. In the same application (production temperature up to 75 °C), Colombo et al. [18] concluded that HFO-1234ze(E) seems the most suitable refrigerant for HTHPs equipped with a semi-hermetic reciprocating compressor, despite its heating capacity reduction.

At a water production temperature of 75 °C, COP of HFO-1234ze(E) was higher than that of its isomer HFO-1234ze(Z) and confirmed its potential for MHTHP [19]. Mota Babiloni et al. [20] concluded that HFO-1234ze(E) was the best mildly flammable alternative for the lower stage of optimised HTHP cascades, reaching temperatures up to 100 °C. Moreover, Arpagaus et al. [21] identified the use of HFO-1234ze(E) in a few large-scale HTHP for heat production up to 95 °C, with piston and turbo compressor technology. Lately, Arpagaus et al. [22] simulations agreed with Mota-Babiloni et al. [20] and confirmed the convenience of using this refrigerant. Mateu-Royo et al. [23] also considered HFO-1234ze(E) a promising alternative in heat pumps for heating production up to 90 °C that uses a district heating network as a heat sink and can be combined with a CO$_2$ transcritical booster for supermarket refrigeration.

Bellair and Hood [24] concluded that HFO-1234ze(E) could be safely handled when appropriate engineering controls are implemented based on a thorough safety risk assessment process. However, this refrigerant is classified as A2L, and safety measures must be considered in the installation and components. The use of a non-flame propagation refrigerant can be advantageous for escalating heat pumps. HFO-1234ze(E) and HFO-1234yf are mixed with other refrigerants to solve this issue, taking advantage of their low GWP values for obtaining refrigerants with intermediate GWP values.

At this moment, most of the registered A1 mixtures are based on

HFO-1234ze(E), Table 1 [25]. The most commonly explored mixture is R-450A, the first HFC/HFO mixture registered and proved its acceptable performance at higher condensing temperatures [25]. R-515B is the mixture with lower GWP from all mixtures included in this table while keeping the A1 safety classification.

R-515B (GWP of 293) is an azeotropic mixture of HFO-1234ze(E) and small amounts of R-227ea. It represents a trade-off refrigerant between mildly flammable HFOs (GWP around 1) and non-flammable medium GWP alternatives [27]. As an azeotropic mixture, it does not present heat transfer performance degradation caused by concentration gradients in phase-change processes proved in refrigerants with notable temperature glide [28]. R-515B has not been identified by many of the current existing works because of its recent development [26,29]. Up to this day, only Bell et al. [30] named this mixture when looking for non-flammable replacements of HFC-134a.

There is a lack of experimental research in low GWP alternatives for HPWH and MHTHP applications, especially in synthetic refrigerants. After a comprehensive screening, a previous article [31] has proved the potential of HFO-1234ze(E) and R-515B for various HFC-134a heat pump applications at moderate and high temperatures theoretically. R-515B is a refrigerant with comparable characteristics to HFO-1234ze(E), and it is the non-flammable alternative with the lowest GWP. However, R-515B has not been considered to replace HFC-134a despite its potential due to safety and environmental characteristics. Therefore, this

Table 1

Composition of A1 alternative mixtures to HFC-134a (adapted from [26]).

Mixture	GWP	HFC-134a	ze[a]	yf[a]	HFC-32	R-125	R-227ea
		Mass in composition, %					
R-450A	605	42.0	58.0				
R-456A	687	45.0	49.0		6.0		
R-460C	766	46.0	49.0		2.5	2.5	
R-513A	631	44.0		56.0			
R-513B	596	41.5		58.5			
R-515A	393		88.0				12.0
R-515B	293		91.1				8.9

[a] ze and yf stand for HFO-1234ze(E) and HFO-1234yf, respectively.

work presents and compares experimental results for the low GWP alternatives HFO-1234ze(E) and its mixture R-515B for confirming the viability of this refrigerant. Different evaporating and condensing temperatures are proposed to cover a wide range of moderately high temperature heat pump applications. A thorough methodology is followed to provide accurate results and ensure repeatability. The most representative experimental measurements and results (mass flow rate, volumetric capacity, heating capacity, compressor power consumption, COP, and discharge temperature) are presented and discussed to justify the convenience of these low GWP alternatives. A match in heating capacity increasing the compressor rotational speed is studied. Finally, the TEWI metric is used to confirm the environmental viability of the proposed alternatives.

2. Short description of the refrigerants selected

This paper validates HFO-1234ze(E) capacity and its new mixture R-515B to replace HFC-134a in HPWH and MHTHP applications. But first, Table 2 introduces these refrigerants by showing their main characteristics. Note that thermodynamic properties have been calculated using REFPROP v10.0 [32]. Detailed discussion about the characteristics of both refrigerants from a thermodynamic point of view is included in [31].

3. Experimental procedure

3.1. Experimental setup

Different operating conditions of HPWH and MHTHP are simulated through a flexible vapour compression experimental setup (Fig. 1). This system is composed of the primary circuit (heat pump) and two secondary (auxiliary) closed loops, which allow setting the operating temperatures and heat transfer in the evaporator and condenser.

Firstly, the heat pump circuit is composed of a frequency-controlled scroll compressor (suction volume of 114.5 cm^3), three plate heat exchangers, evaporator, condenser, and internal heat exchanger (IHX), with total heat exchange areas of 2.39, 1.39, and 0.336 m^2 by using 40, 24 and 30 plates, respectively; and an electronic expansion valve, as main elements. It includes other components required for ensuring proper operation of the system such as filter dryer, manual and solenoid valves, liquid receiver (7.1 dm^3 capacity), and other safety devices

(pressure switch, pressure release valve, etc.). 3.25 dm^3 of POE oil has been used as the lubricant (32 cP viscosity). It has proved compatibility with previous HFO-1234ze(E) mixtures (R-450A) in the same installation [34].

The evaporator secondary circuit (load circuit) uses a commercial brine (glycol/water) as the heat transfer fluid, which is heated by three 5.6 kW resistances (one of them PID controlled through the software) immersed in a 100 L tank. It also includes a water pump with a frequency inverter and other components. The condenser secondary circuit (dissipation circuit) includes a PID controlled fan coil, a water pump with a frequency inverter, and other components.

Measurement instruments are a Coriolis mass flow meter in the heat pump circuit ($\pm 0.1\%$, reading), volumetric flow meters in the secondary circuits ($\pm 0.33\%$, reading for the dissipation circuit, and ± 0.114 m^3 h^{-1} for the load circuit). Moreover, the test rig includes K type thermocouples at the inlet and outlet of the main components of all circuits (± 0.3 K). Pressure transducers at the inlet and outlet of the main components of heat pump circuits ($\pm 0.15\%$, reading) are also used. Finally, the power consumption uncertainty is $\pm 1.55\%$, reading.

3.2. Experimental tests

Several values of evaporating and condensing temperatures have been proposed for studying the most representative operating range of HPWH and MHTHP applications. Moreover, particular attention has been devoted to the maximum suction and discharge temperatures allowed for the compressor, 50 and 150 °C, respectively. Considering the applications of interest, temperatures finally selected were 7.5, 15 and 22.5 °C for evaporation and from 55 to 85 °C at intervals of 5 °C for condensation (a total of 55 experimental tests). Due to higher discharge temperatures of HFC-134a, the maximum condensing temperature allowed for this refrigerant was 75 °C.
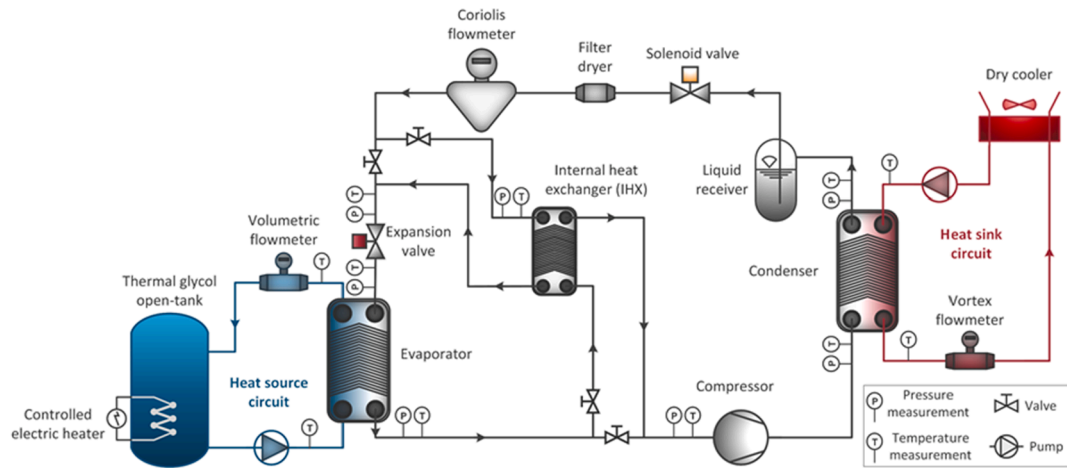
All tests were performed considering the same compressor frequency (rotational speed of 2030 rpm). However, additional tests with increased compressor frequency have been carried out to observe the results with a capacity matching between the alternatives and HFC-134a. The validation was performed at the intermedium evaporating temperature, 15 °C, and condensing temperatures from 55 to 75 °C (10 additional tests).

The theoretical IHX effect on the installation has been simulated before the test campaign. It has been proved that the heating performance benefit is slight and can cause problems with discharge temperature. Consequently, the total superheating degree has been limited to 20 K, corresponding to 15 K of that to the superheating caused by the IHX. This value limits the suction/discharge temperature at the values previously mentioned and prevents the compressor from damage. The IHX operation directly sets the total subcooling degree since this experimental setup is equipped with a liquid receiver. The internal heat exchanger effectiveness was adjusted as explained in [34].
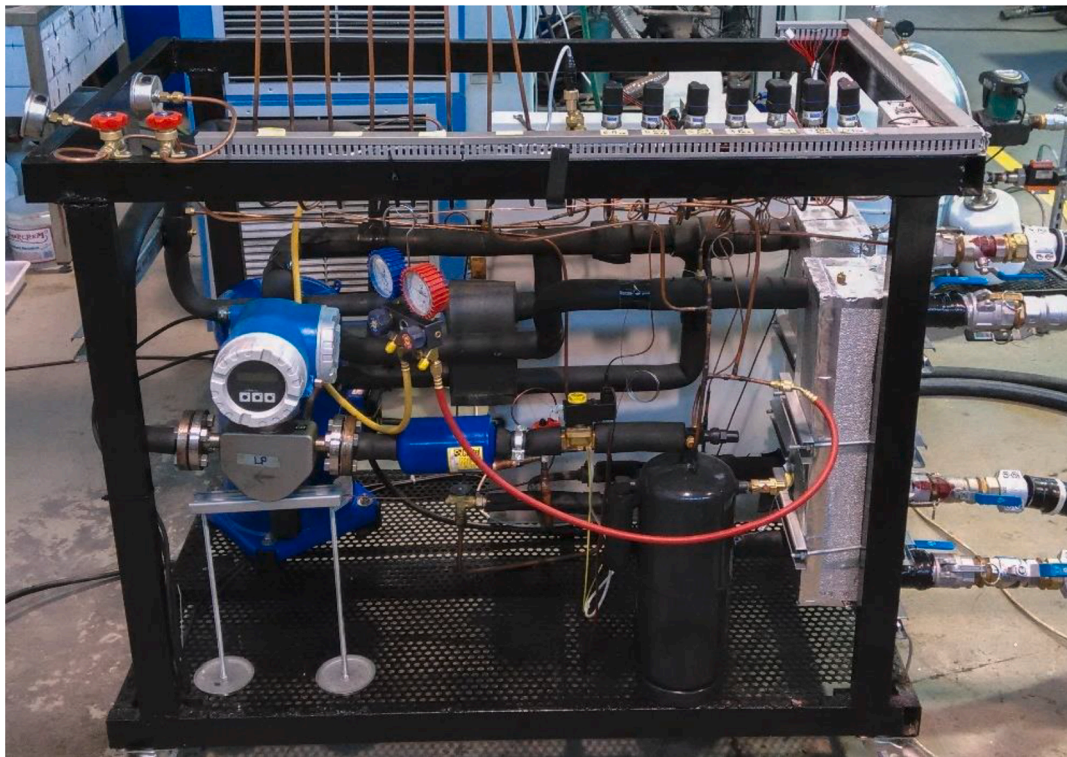
The refrigerant charge is 7.5 kg (cannot be optimised because of the liquid receiver). Then, the volumetric flow rate in the secondary circuits was adjusted in the pumps for reaching a temperature difference of 12.5 K and 20 K in the evaporator (glycol brine) and condenser (water), respectively.

Robust PID controllers have been defined for reaching targeted operating temperatures in both secondary circuits and then allowing a minimum deviation once the steady-state test is recorded. While the PID controlled the fan coil frequency to control condensation temperature, a PID controlled resistance set the evaporation temperature. The PID of the electronic expansion valve has also been manually modified for proper operation. The minimum human intervention and higher automation of tests during the tests allow higher accuracy in the experimental results.

Each test was recorded for a minimum of 20 min, being 5 s the measurement period. A Python program selected the most convenient 5 min period (it considers standard deviation and proximity to target

Table 2
Main characteristics of the refrigerants tested.

Parameters	HFC-134a	HFO-1234ze (E)	R-515B
Molecular weight (g·mol^{-1})	102.0	114.0	119.0
Critical temperature (°C)	101.1	109.4	108.7
Critical pressure (MPa)	4.06	3.64	3.56
Normal boiling point (NBP) (°C)	−26.10	−18.95	−18.89
Condensing pressure[a] (MPa)	2.12	1.61	1.60
Vapour pressure[c] (MPa)	0.66	0.50	0.50
Latent heat of vaporization[b] (kJ·kg^{-1})	163.0	154.8	148.2
Latent heat of condensation[a] (kJ·kg^{-1})	124.4	123.8	118.2
Suction density[b] (kg·m^{-3})	50.09	40.64	42.08
Liquid/Vapour density[a] (kg·m^{-3})	996.3/115.6	986.2/91.6	1006.3/95.1
Liquid/Vapour specific heat[a] (kJ·kg^{-1}·K^{-1})	1.80/1.61	1.65/1.33	1.62/1.32
Specific heat ratio[b]	1.61	1.55	1.54
ODP (CFC-11 = 1) [33]	0	0	0
GWP$_{100\text{-years}}$ [33]	1430	<1	299
ASHRAE Std. 34 safety class [33]	A1	A2L	A1

[a] At temperature saturated conditions of 70 °C.
[b] At temperature saturated conditions of 40 °C.
[c] At ambient temperature of 25 °C.

a)

b)

Fig. 1. Experimental setup: a) schematic diagram and b) picture of the main circuit.

temperatures). Therefore, the average value of 60 measurements has been used to define each parameter's value at the selected operating temperature. The refrigerants' thermodynamic states are calculated using REFPROP v10.0 [32], as indicated in Section 2.

3.3. Equations

The heating capacity at the refrigerant side, Eq. (1), is the product of the measured refrigerant mass flow rate ($\dot{m}_{ref}$) and the heating effect, calculated as the enthalpy at the condenser inlet ($h_{k,in}$) and outlet ($h_{k,out}$).

$$\dot{Q}_{k,ref} = \dot{m}_{ref}\left(h_{k,in} - h_{k,out}\right) \tag{1}$$

On the other hand, the heating capacity at the water side is obtained using the water mass flow rate ($\dot{m}_{water}$), specific heat, and the temperature difference between the condenser outlet ($T_{water,out}$) and inlet ($T_{water,in}$), as in Eq. (2).

$$\dot{Q}_{k,water} = \dot{m}_{water}c_{p,water}\left(T_{water,out} - T_{water,in}\right) \tag{2}$$

The heat exchanger's effectiveness is calculated using Eq. (3) to control the total superheating degree of the installation.

$$\varepsilon_{IHX} = \frac{h_{suc} - h_{ev,out}}{h_{k,out} - h_{ev,out}} \tag{3}$$

The COP is the ratio of the heating capacity and the measured compressor power consumption, Eq. (4).

$$COP = \frac{\dot{Q}_k}{\dot{W}_c} \tag{4}$$

The compressor global and volumetric efficiencies are determined through Eq. (5) and (6). The volumetric compressor efficiency is calculated using the refrigerant mass flow rate and parameters from this component. The compressor efficiency takes into account isentropic and electromechanical efficiencies and the consumption of the compressor ($\dot{W}_c$), mass flow rate and isentropic work of compression are used for its calculation.

$$\eta_{vol} = \frac{\dot{m}_{ref}}{\rho_{suc} V_c \left(\frac{N}{60} \right)} \tag{5}$$

$$\eta_c = \frac{\dot{m}_{ref} \Delta h_{is,c}}{\dot{W}_c} \tag{6}$$

3.4. Validation of experiments

Heating capacities at the refrigerant and water sides are compared to obtain the condenser heat balance. This balance allows checking the validity of experimental measurements and calculations. Fig. 2 proves that all points fall into the $\pm$ 10% range, being the difference in results between R-515B and the rest justified by the variation of the secondary mass flow rate for water temperature difference adjustment.

Operating at discharge temperatures close to the limit can degrade the lubricant oil. This malfunction is visible because it causes a variation in operational and energetic parameters such as discharge temperature or compressor, respectively. Therefore, one test was selected for validation of the results. Condensation and evaporation temperatures of 65 °C and 15 °C were tested at the beginning and the end of the experimental campaign with each refrigerant. Moreover, even though a pressure test was performed with nitrogen before the first experimental campaign, repeatability tests also help check that the system does not noticeably leak refrigerant. Table 3 shows the difference between the validation tests for some representative parameters.

3.5. Uncertainty propagation

The uncertainty propagation is fundamental in the experimental studies that illustrate a certain confidence level in the results. Although random errors are not reproducible and cannot be corrected, the measurements often exhibit the characteristics of normally distributed events. Therefore, these errors can be characterised by statistical methods. In general, the series of measurements extracted from the statistical population can be described as indicated in Eq. (7).

$$\bar{x} \pm \sigma_x \tag{7}$$

Where $\bar{x}$ is the arithmetic average and σ_x is the empirical standard deviation. Then, in Eq. (8), i indicates the measurement, and n is the
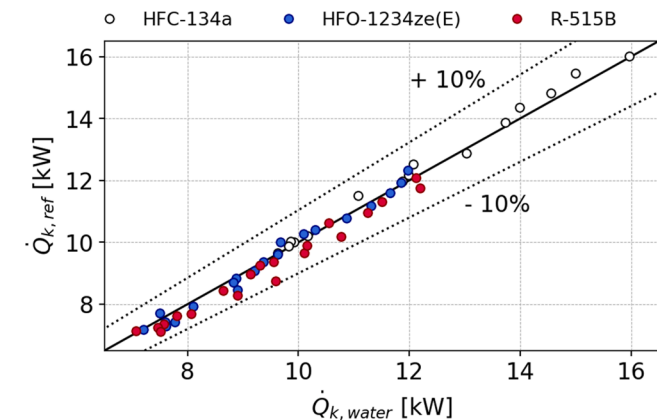
Table 3
Deviation of selected parameters for the validation test ($T_k = 15$ °C and $T_o = 65$ °C).

Refrigerant	HFC-134a	HFO-1234ze(E)	R-515B
Discharge Temperature (K)	0.14	0.02	1.23
Refrigerant mass flow rate (%)	0.25	0.15	0.35
Heating capacity (%)	0.41	0.86	0.60
Compressor power consumption (%)	0.67	0.57	0.15
COP (%)	0.24	0.24	0.45

number of measurements.

$$\sigma_x = \sqrt{\frac{1}{n-1} \sum_{i=1}^{n} (x_i - \bar{x})^2} \tag{8}$$

Although the confidence interval of the arithmetic average and the empirical standard deviation is 68.3%, the empirical standard deviation is multiplied by 2 to obtain a confidence level of 95.5%.

Nevertheless, as parameters of interest cannot be measured directly, they are derived from others such as temperature and pressure. Thus, the Gaussian law of error propagation can be applied to quantify the uncertainty of the derived parameters. When the quantity desired Y is calculated as a function of one or more variables from direct measurement, $Y = f(x_1, x_2, x_3, \cdots, x_k)$, the standard deviation of the derived quantity is described by Eq. (9).

$$\sigma_y = \sqrt{\sum_{j=1}^{k} \left(\frac{\partial Y}{\partial x_j} \right)^2 \overline{\sigma}_x^2} \tag{9}$$

Where the index j describes the influencing variables of the derived quantity Y. The software EES [35] has been used to implement the partial derivative of a function. It is required to calculate the uncertainty of the desired quantity with that of the measured quantities.

4. Results and discussion

4.1. Operating and energetic performance

In this section, the results measured or calculated from experimental tests have been presented and discussed. The X-axis represents the different condensing temperatures tested, colours evidence each refrigerant, and symbols highlight evaporating levels. When compressor efficiencies are discussed, results included in Figures are represented against pressure ratio, without distinction of evaporating or condensing temperatures.

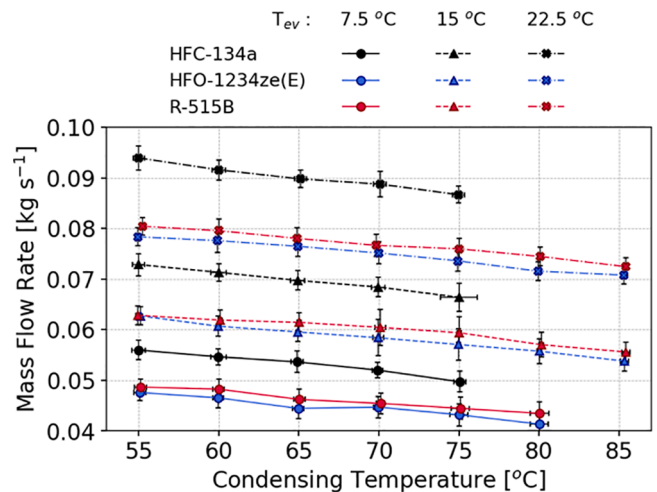The first parameter presented in the paper is the mass flow rate,

Fig. 2. Heating capacity balance.

Fig. 3. Mass flow rate experimental measurements.

directly measured from the mass flow meter, Fig. 3. Both alternatives present a significant reduction from HFC-134a results, being HFO-1234ze(E) the refrigerant with the lowest values in most situations. Therefore, the use of R-515B causes an average mass flow rate decrease of 13% and HFO-1234ze(E) of 15%, both compared to HFC-134a.

The mass flow rate is proportional to compressor suction density. Therefore, the enormous difference in this value (Table 1) explains the noticeable difference in mass flow rate and the evolution with varying evaporating temperature at constant superheating degree and compressor rotational speed. However, this difference is lower than expected because both alternatives' volumetric compressor efficiency is higher than HFC-134a. As Fig. 4 exposes, the volumetric efficiency of HFO-1234ze(E) is higher than R-515B at lower pressure ratios, whereas the difference between both alternatives is reduced when increasing this parameter. On average, the alternatives' volumetric efficiency is 4% higher than HFC-134a even though the compression ratio for the same operating conditions is increased approx. 2%.

Before discussing heating capacity results, the experimental heating effect is shown in Fig. 5. At low evaporating temperatures, the effect of condensing temperature is positive concerning this value. Similarly, as seen with the mass flow rate, the heating effect of HFC-134a is higher than that of alternatives. For HFO-1234ze(E), the reduction is 8% to 12% higher at low evaporating temperatures and 7% to 8%. For R-515B instead, the reduction is from 12% to 16% and from 11% to 12%, respectively). The higher HFC-134a latent heat of condensation and enthalpy at compressor discharge at the same operating conditions explains this phenomenon.

Once analysed, both parameters that proportionally affect heating capacity (heating effect and mass flow rate) are depicted in Fig. 6. As expected, the low GWP refrigerants cause a significant reduction of the heating capacity delivered, ranging from 22% to 25% for HFO-1234ze (E) and from 23% to 27% for R-515B. If heating capacity is a critical parameter, a variable speed compressor or a unit redesign with a grater compressor displacement is recommended to keep these values at HFC-134a levels. Suppose the heat pump unit is used as a waste heat valorisation system. In that case, this can cause higher requirements from the main heating system or longer charging periods for the heat accumulator/battery.

Before assessing the energy performance results based on the COP, the compressor power consumption is analysed. Fig. 7 exhibits the experimental measurements for this parameter. A smaller influence of the evaporating temperature is seen because the mass flow rate almost offsets the variation of the specific work of compression. Consequently, the compressor power consumption is slightly lower at higher evaporating temperatures. On the contrary, compressor power consumption grows with the increase of condensing temperature since the pressure ratio augments the specific compression work.

Regarding the refrigerant comparison, the compressor consumes less power using both alternatives. Even though the difference is minimum,
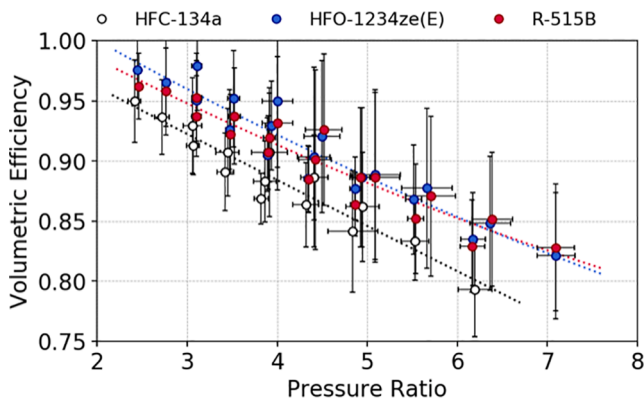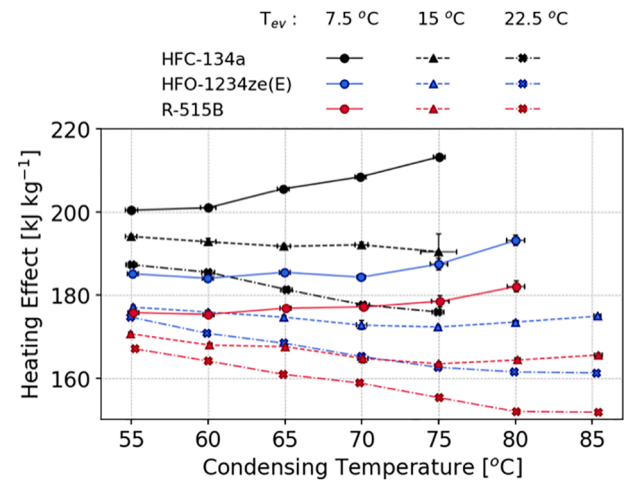
Fig. 5. Heating effect experimental results.
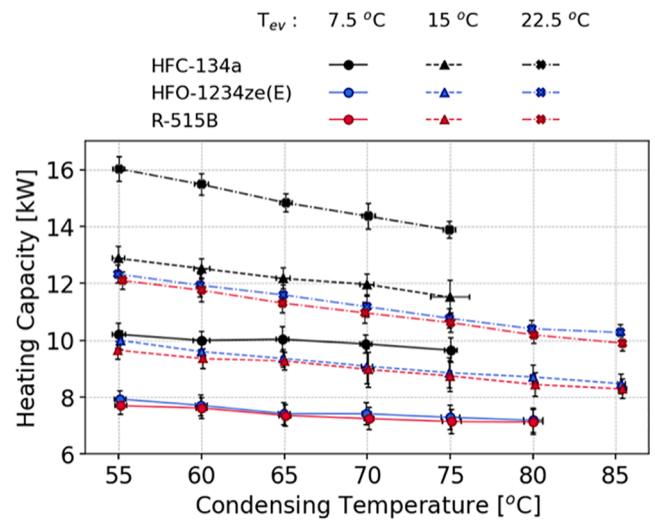
Fig. 6. Heating capacity experimental results.

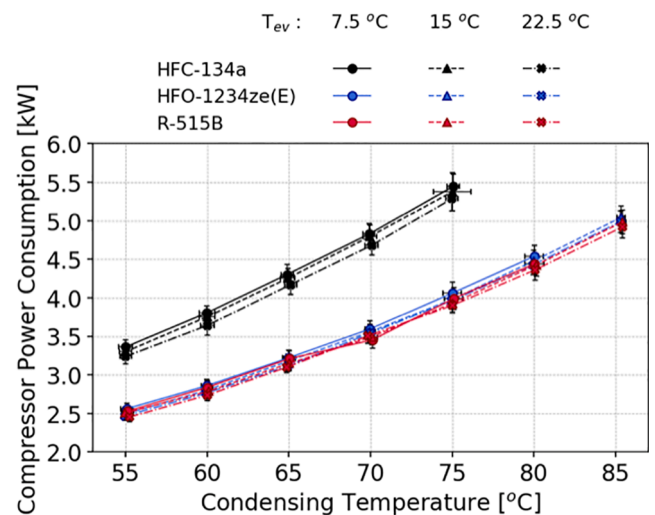**Fig. 7.** Compressor power consumption experimental measurements.

Fig. 4. Compressor volumetric efficiency experimental results.

R-515B is the refrigerant with the lowest values measured. The difference between HFC-134a and the alternatives is, on average, 25%.

Overall compressor efficiency is calculated from compressor power consumption, and these results are included in Fig. 8. As happened for volumetric efficiency, HFO-1234ze(E) results in slightly higher average values, particularly at lower pressure ratios. The difference compared to HFC-134a is increased at higher pressure ratios. On average, the volumetric efficiency of HFO-1234ze(E) and R-515B is 4% and 3% higher than that of HFC-134a, respectively. Therefore, considering the resulting compressor efficiencies observed, it can be concluded that both alternatives appropriately adapt to HFC-134a scroll compressors and lubricants.

The last energetic parameter analysed is the (heating) coefficient of performance (COP), which results are included in Fig. 9. The three refrigerants present comparable results in COP, so the difference in heating capacity and compressor power consumption is a similar level. The only remarkable difference is the lower COP of HFC-134a at higher condensing temperatures (note that it is the refrigerant with the lowest critical temperature). Overall, the conclusion regarding COP is that the replacement of HFC-134a with HFO-1234ze(E) or R-515B does not cause a noticeable variation in the performance of the heat pump (average is 2% and 1%, respectively), except at higher condensation temperatures (MHTHP conditions), where the COP increase can reach up to 5% for HFO-1234ze(E) and 4% for R-515B. These results confirm predictions made by the theoretical analysis of [31] for most conditions and even surpass what has been expected at higher condensation temperatures.

Finally, discharge temperatures are included in Fig. 10. It can be seen why HFC-134a experimental tests could not reach higher condensing temperatures because its values are 10 and 11 K higher than that of HFO-1234ze(E) and R-515B, respectively. HFC-134a reaches 145 °C at 75 °C condensing temperature and 7.5 °C evaporating temperature, and at this point, that of alternatives is around 20 K lower. It is also proved how these low GWP alternatives help extend the operating range of heat pumps or extend the installation's lifetime at the same operating conditions. Moreover, R-515B could even reduce discharge temperature a few degrees over HFO-1234ze(E) while improving the unit's safety.

4.2. Heating capacity matching

As exposed in Section 3.2 and attending to the interesting conclusions drafted in [36], this section includes the results for which compressor frequency has been increased when using HFO-1234ze(E) and R-515B to match HFC-134a heating capacity. The theoretical compressor frequency required has been calculated and then set in additional experimental tests. The resulting theoretical frequency for matching in heating capacity is 48.3 Hz on average, and these results are compared with those of HFC-134a at 35 Hz. An intermediate evaporation temperature between the HPHW and MHTHP has been fixed.
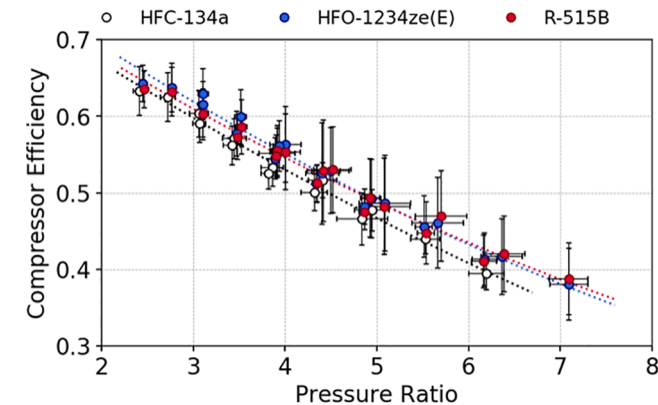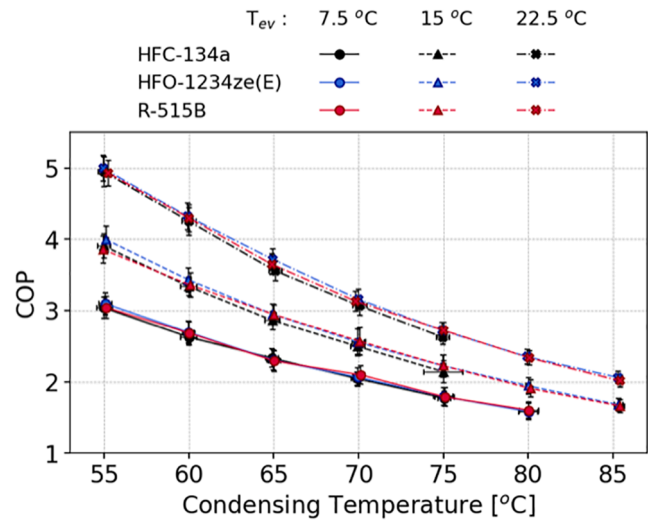
Fig. 9. Coefficient of Performance (COP) experimental results.
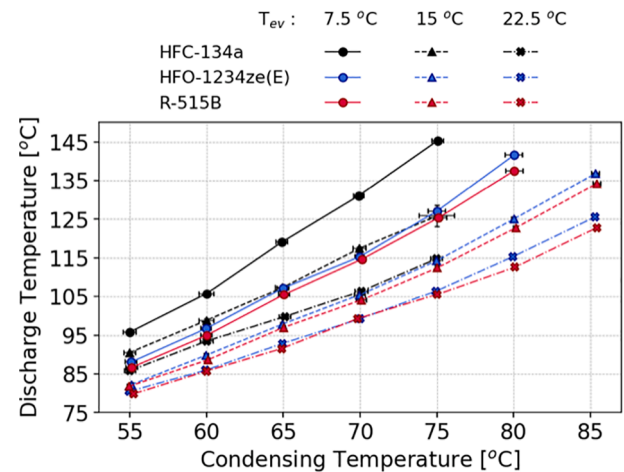
Fig. 10. Discharge temperature experimental measurements.

In this regard, Fig. 11.a) shows the resulting heating capacity. As before, HFO-1234ze(E) heating capacity remains above R-515B, matching HFC-134a or slightly higher. At this compressor frequency, the heating capacity of R-515B is still before that of HFC-134a and would require a higher value. Then, Fig. 11.b) shows positive results for the COP of both alternatives. Except for the lowest condensing temperature condition, COP of HFO-1234ze(E) and R-515B is higher than HFC-134a. While HFO-1234ze(E) benefits from lower condensing temperatures, R-515B matches or even surpass HFC-134a COP from 70 °C.

4.3. Carbon footprint analysis

Finally, a carbon footprint analysis is proposed to validate a part of the environmental benefit of substituting HFC-134a with low GWP alternatives. Total Equivalent Warming Impact (TEWI) is the metric selected for obtaining the reduction in carbon dioxide equivalent (CO_2e) emissions because it does not require many assumptions, and the accuracy is comparable to other more complex analysis [37].

Following this work's recommendations, different scenarios are proposed, considering various situations in a heat pump. Therefore, two carbon emission factors (electricity generation primarily based on renewable sources, Sweden, or fossil fuels, Germany) and two leakage rates (representing situations of proper or low maintenance) are considered in the analysis. The TEWI metric is calculated as indicated in
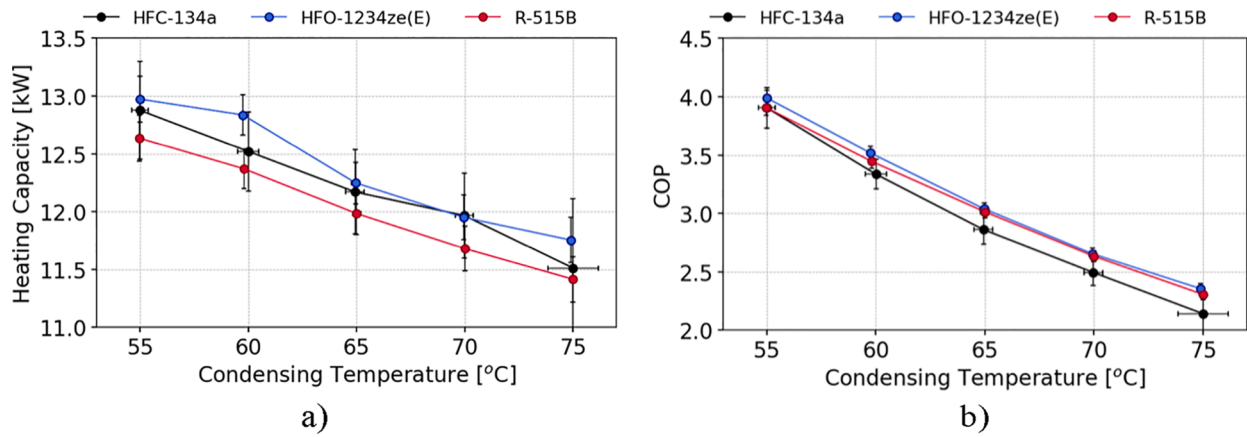
Fig. 8. Overall compressor efficiency experimental results.

Fig. 11. Experimental results for a) heating capacity and b) COP, with frequency increased for the alternatives.

Eq. (7).

$$TEWI = GWP \cdot m_{ref} \cdot L \cdot n + GWP \cdot m_{ref} \cdot (1 - \alpha) + n \cdot E_a \cdot \beta \tag{7}$$

Fig. 12 contains results for the possible TEWI reduction caused by the replacement of HFC-134a by HFO-1234ze(E) and R-515B, considering two different operating conditions, HPWH and MHTHP, setting the evaporating temperature at 7.5 and 22.5 °C, and condensing temperature at 60 and 75 °C, respectively.

The alternatives' carbon footprint reduction is evident, primarily affected by the refrigerant leak in countries with lower emission factors, such as Denmark or Sweden. In countries with emission factor at the level of Germany or considering the EU's average, the maximum reduction (at 25% refrigerant leak) is between 15% and 28% for both alternatives. Moreover, environmental benefit conditions of MHTHP

(higher condensing temperature) seem more advantageous than the HPWH mode. Although TEWI reduction produced using R-515B is lower than that of HFO-1234ze(E), the environmental benefit is still incontestable, helping extend safer large capacity heat pump systems.

5. Conclusions

The interest in heat pumps is rising in the past years, as these systems are considered clean technologies because they can be powered by renewable energy. Heat pump water heater and moderately high temperature heat pumps are applications with moderate temperature levels (55 to 85 °C) which refrigerants have not been yet studied in deep. The low GWP HFO-1234ze(E) and an up-and-coming non-flammable mixture named R-515B are experimentally studied from operational,
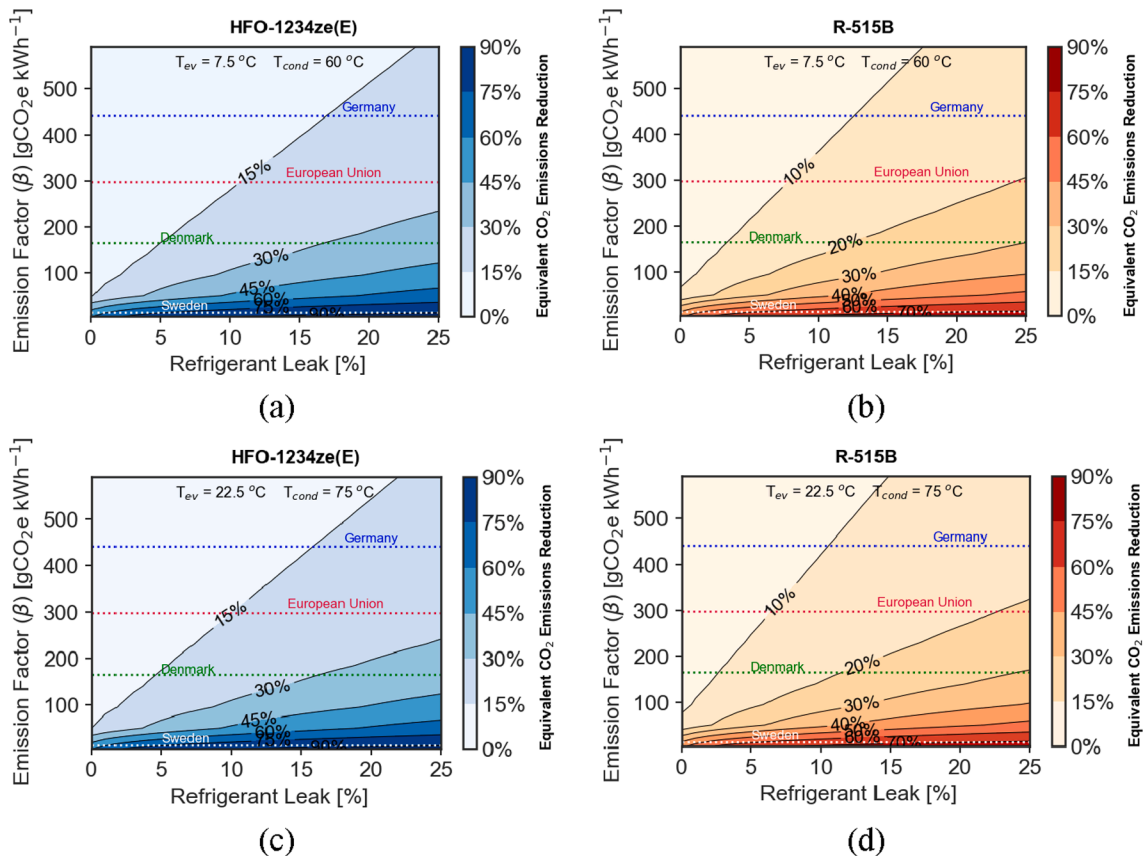

Fig. 12. TEWI reduction using low GWP alternatives instead of HFC-134a.

energetic, and environmental perspectives to replace HFC-134a.

65 experimental tests have been performed at condensing temperatures between 55 and 85 °C, and evaporating temperatures between 7.5 and 22.5 °C in a heat pump experimental setup equipped with a scroll compressor. The main conclusions are as follows:

- The mass flow rate of HFO-1234ze(E) and R-515B is significantly decreased compared to HFC-134a, being 15% and 13% lower, respectively. The suction density causes this diminution, considering that the volumetric efficiency of alternatives results is around 4% higher.

- The heating effect of alternatives is also diminished. Consequently, the alternatives' heating capacity remains below that of R-134a, down to 25% and 27% in the case of HFO-1234ze(E) and R-515B.

- The deviation in compressor power consumption follows a similar behaviour, motivated by a slightly higher compressor overall efficiency, and alternatives have comparable or higher COP. At higher condensation (heat production/sink) temperatures, the alternatives increase COP up to 5%. Discharge temperatures of alternatives can be 20 K lower, which allows extending the tests up to 85 °C condensation temperatures.

- If heating capacity requirements are strict, a new installation, compressor, or higher frequency would require the proposed alternatives. In this way, the average frequency for matching HFC-134a in heating capacity was theoretically assessed, 48.3 Hz. At 15 °C evaporation temperature and increased frequency, HFO-1234ze(E) match heating capacity while increasing COP. R-515B heating capacity remains below that of HFC-134a even though it is close to the match.

- The carbon footprint (TEWI) analysis reveals that both fluids can significantly benefit from an environmental perspective in situations with lower emission factors. Environmental benefits do not vary significantly between HTHP and MHTHP applications, even though benefits are lightly more noticeable in the second situation.

This work confirms that HFO-1234ze(E) and R-515B do not cause noticeable differences in operational or energetic parameters. There would be energetic benefits, an extended operating range, and carbon emissions reduced in both situations. This paper provides a significant amount of experimental information that could be combined with that shown by [18] and that included in previous refrigeration systems [14] to understand better the HFO-1234ze(E) behaviour in heat pumps.

Declaration of Competing Interest

The authors declare that they have no known competing financial interests or personal relationships that could have appeared to influence the work reported in this paper.

Acknowledgements

References

[1] F. Schlosser, M. Jesper, J. Vogelsang, T.G. Walmsley, C. Arpagaus, J. Hesselbach, Large-scale heat pumps: Applications, performance, economic feasibility and industrial integration, Renew. Sustain. Energy Rev. 133 (2020), 110219, https://doi.org/10.1016/j.rser.2020.110219.

[2] A. Mota-Babiloni, J. Navarro-Esbrí, Á. Barragán-Cervera, F. Molés, B. Peris, G. Verdú, Commercial refrigeration - An overview of current status, Int. J. Refrig. 57 (2015), https://doi.org/10.1016/j.ijrefrig.2015.04.013.

[3] M. Karampour, S. Sawalha, State-of-the-art integrated CO2 refrigeration system for supermarkets: A comparative analysis, Int. J. Refrig. 86 (2018) 239–257, https://doi.org/10.1016/J.IJREFRIG.2017.11.006.

[4] J.M.M. Belman-Flores, J.M.M. Barroso-Maldonado, A.P.P. Rodríguez-Muñoz, G. Camacho-Vázquez, Enhancements in domestic refrigeration, approaching a sustainable refrigerator - A review, Renew. Sustain. Energy Rev. 51 (2015) 955–968, https://doi.org/10.1016/j.rser.2015.07.003.

[5] I. Sarbu, A review on substitution strategy of non-ecological refrigerants from vapour compression-based refrigeration, air-conditioning and heat pump systems, Int. J. Refrig. 46 (2014) 123–141, https://doi.org/10.1016/j.ijrefrig.2014.04.023.

[6] N. Deng, X. Jing, R. Cai, J. Gao, C. Shen, Y. Zhang, H. Sui, Molecular simulation and experimental investigation for thermodynamic properties of new refrigerant NBY-1 for high temperature heat pump, Energy Convers. Manag. 179 (2019) 339–348, https://doi.org/10.1016/J.ENCONMAN.2018.10.076.

[7] G.F. Frate, L. Ferrari, U. Desideri, Analysis of suitability ranges of high temperature heat pump working fluids, Appl. Therm. Eng. 150 (2019) 628–640, https://doi.org/10.1016/J.APPLTHERMALENG.2019.01.034.

[8] X. Wu, Z. Xing, Z. He, X. Wang, W. Chen, Performance evaluation of a capacity-regulated high temperature heat pump for waste heat recovery in dyeing industry, Appl. Therm. Eng. 93 (2016) 1193–1201, https://doi.org/10.1016/j.applthermaleng.2015.10.075.

[9] M. Arnaudo, F. Giunta, J. Dalgren, M. Topel, S. Sawalha, B. Laumert, Heat recovery and power-to-heat in district heating networks – A techno-economic and environmental scenario analysis, Appl. Therm. Eng. 185 (2021), 116388, https://doi.org/10.1016/j.applthermaleng.2020.116388.

[10] United Nations Environment Programme (UNEP), Twenty-Eighth Meeting of the Parties to the Montreal Protocol on Substances that Deplete the Ozone Layer. Decision XXVIII/— Further Amendment of the Montreal Protocol., (2016) 1–9.

[11] J. Sieres, I. Ortega, F. Cerdeira, E. Álvarez, Drop-in performance of the low-GWP alternative refrigerants R452B and R454B in an R410A liquid-to-water heat pump, Appl. Therm. Eng. 182 (2021), 116049, https://doi.org/10.1016/j.applthermaleng.2020.116049.

[12] B. Kim, D.C. Lee, S.H. Lee, Y. Kim, Performance assessment of optimized heat pump water heaters using low-GWP refrigerants for high- and low-temperature applications, Appl. Therm. Eng. (2020), https://doi.org/10.1016/j.applthermaleng.2020.115954.

[13] A. Mota-Babiloni, P. Makhnatch, R. Khodabandeh, Recent investigations in HFCs substitution with lower GWP synthetic alternatives: Focus on energetic performance and environmental impact, Int. J. Refrig. 82 (2017) 288–301, https://doi.org/10.1016/j.ijrefrig.2017.06.026.

[14] A. Mota-Babiloni, J. Navarro-Esbrí, F. Molés, Á.B. Cervera, B. Peris, G. Verdú, A review of refrigerant R1234ze(E) recent investigations, Appl. Therm. Eng. 95 (2016), https://doi.org/10.1016/j.applthermaleng.2015.09.055.

[15] Y. He, Y. Jiang, Y. Fan, G. Chen, L. Tang, Utilization of ultra-low temperature heat by a novel cascade refrigeration system with environmentally-friendly refrigerants, Renew. Energy. 157 (2020) 204–213, https://doi.org/10.1016/j.renene.2020.05.018.

[16] G.A. Longo, S. Mancin, G. Righetti, C. Zilio, R1234yf and R1234ze(E) as environmentally friendly replacements of R134a: Assessing flow boiling on an experimental basis, Int. J. Refrig. 108 (2019) 336–346, https://doi.org/10.1016/j.ijrefrig.2019.09.008.

[17] K. Nawaz, B. Shen, A. Elatar, V. Baxter, O. Abdelaziz, R1234yf and R1234ze(E) as low-GWP refrigerants for residential heat pump water heaters, Int. J. Refrig. 82 (2017) 348–365, https://doi.org/10.1016/j.ijrefrig.2017.06.031.

[18] L.P.M. Colombo, A. Lucchini, L. Molinaroli, Experimental analysis of the use of R1234yf and R1234ze(E) as drop-in alternatives of R134a in a water-to-water heat pump, Int. J. Refrig. (2020), https://doi.org/10.1016/j.ijrefrig.2020.03.004.

[19] S. Fukuda, C. Kondou, N. Takata, S. Koyama, Low GWP refrigerants R1234ze(E) and R1234ze(Z) for high temperature heat pumps, Int. J. Refrig. 40 (2014) 161–173, https://doi.org/10.1016/j.ijrefrig.2013.10.014.

[20] A. Mota-Babiloni, C. Mateu-Royo, J. Navarro-Esbrí, F. Molés, M. Amat-Albuixech, Á. Barragán-Cervera, Optimisation of high-temperature heat pump cascades with internal heat exchangers using refrigerants with low global warming potential, Energy. 165 (2018) 1248–1258, https://doi.org/10.1016/j.energy.2018.09.188.

[21] C. Arpagaus, F. Bless, M. Uhlmann, J. Schiffmann, S.S. Bertsch, High temperature heat pumps: Market overview, state of the art, research status, refrigerants, and application potentials, 2018. https://www.sciencedirect.com/science/article/pii/S0360544218305759 (accessed April 27, 2018).

[22] C. Arpagaus, M. Prinzing, R. Kuster, F. Bless, M. Uhlmann, J. Schiffmann, S.S. Bertsch, High temperature heat pumps -Theoretical study on low GWP HFO and HCFO refrigerants, in: ICR 2019, 25th IIR Int. Congr. Refrig. August 24-30, Montréal, Québec, Canada, 2019: pp. 1–8. doi:10.18462/iir.icr.2019.259.

[23] C. Mateu-Royo, S. Sawalha, A. Mota-Babiloni, J. Navarro-Esbrí, High temperature heat pump integration into district heating network, Energy Convers. Manag. 210 (2020), 112719, https://doi.org/10.1016/j.enconman.2020.112719.

[24] R.J. Bellair, L. Hood, Comprehensive evaluation of the flammability and ignitability of HFO-1234ze, Process Saf. Environ. Prot. 132 (2019) 273–284, https://doi.org/10.1016/j.psep.2019.09.033.

[25] P. Makhnatch, A. Mota-Babiloni, A. López-Belchí, R. Khodabandeh, R450A and R513A as lower GWP mixtures for high ambient temperature countries: Experimental comparison with R134a, Energy. 166 (2019) 223–235, https://doi.org/10.1016/j.energy.2018.09.001.

[26] P. Makhnatch, New refrigerants for vapour compression refrigeration and heat pump systems, KTH Royal Institute of Technology, 2019. http://www.diva-portal.org/smash/get/diva2:1347734/FULLTEXT01.pdf.

[27] BITZER Kühlmaschinenbau GmbH, Refrigerant Report 20, Sindelfingen (Germany), 2018. https://www.bitzer-refrigerantreport.com/fileadmin/user_upload/A-501-20.pdf.

[28] T.A. Jacob, E.P. Matty, B.M. Fronk, Comparison of R404A condensation heat transfer and pressure drop with low global warming potential replacement candidates R448A and R452A, Int. J. Refrig. 116 (2020) 9–22, https://doi.org/10.1016/j.ijrefrig.2020.03.014.

[29] Y. Heredia-Aricapa, J.M.M. Belman-Flores, A. Mota-Babiloni, J. Serrano-Arellano, J.J.J. García-Pabón, Overview of low GWP mixtures for the replacement of HFC refrigerants: R134a, R404A and R410A, Int. J. Refrig. 111 (2020) 113–123, https://doi.org/10.1016/j.ijrefrig.2019.11.012.

[30] I.H. Bell, P.A. Domanski, M.O. McLinden, G.T. Linteris, The hunt for nonflammable refrigerant blends to replace R-134a, Int. J. Refrig. 104 (2019) 484–495, https://doi.org/10.1016/j.ijrefrig.2019.05.035.

[31] C. Mateu-Royo, A. Mota-Babiloni, J. Navarro-Esbrí, Á. Barragán-Cervera, Comparative analysis of HFO-1234ze(E) and R-515B as low GWP alternatives to HFC-134a in moderately high temperature heat pumps, Int. J. Refrig. 124 (2021) 197–206, https://doi.org/10.1016/j.ijrefrig.2020.12.023.

[32] E.W. Lemmon, I.H. Bell, M.L. Huber, M.O. McLinden, NIST Standard Reference Database: Reference Fluid Thermodynamic and Transport Properties-REFPROP, Version 10, Natl. Inst. Stand. Technol. Stand. Ref, Data Program, Boulder, CO, 2018.

[33] Am. Soc. Heating, Refrig. Air-Conditioning Eng. (2017).

[34] V. Pérez-García, A. Mota-Babiloni, J. Navarro-Esbrí, Influence of operational modes of the internal heat exchanger in an experimental installation using R-450A and R-513A as replacement alternatives for R-134a, Energy. 189 (2019), https://doi.org/10.1016/j.energy.2019.116348.

[35] S. Klein, Engineering Equation Solver (EES) V10.2., Fchart Software, Madison, USA Www, Fchart. Com. (2006).

[36] A. Mota-Babiloni, J. Navarro-Esbrí, J.M.J.M. Mendoza-Miranda, B. Peris, Experimental evaluation of system modifications to increase R1234ze(E) cooling capacity, Appl. Therm. Eng. 111 (2017), https://doi.org/10.1016/j.applthermaleng.2016.09.175.

[37] A. Mota-Babiloni, J.R. Barbosa, P. Makhnatch, J.A. Lozano, Assessment of the utilization of equivalent warming impact metrics in refrigeration, air conditioning and heat pump systems, Renew. Sustain. Energy Rev. 129 (2020), 109929, https://doi.org/10.1016/j.rser.2020.109929.